Electronic Supplementary Information (ESI)

Enhanced Luminescence of $Au_{22}(SG)_{18}$ Nanoclusters via Rational Surface Engineering

Kyunglim Pyo‡[a], Viraj Dhanushka Thanthirige‡[b], Sook Young Yoon[a], Guda Ramakrishna[b*] and Dongil Lee[a*]

[a]Department of Chemistry, Yonsei University, Seoul 120-749, Korea
[b]Department of Chemistry, Western Michigan University, Kalamazoo MI 49008, USA
‡ Authors of equal contribution

[*] E-mail : dongil@yonsei.ac.kr, rama.guda@wmich.edu

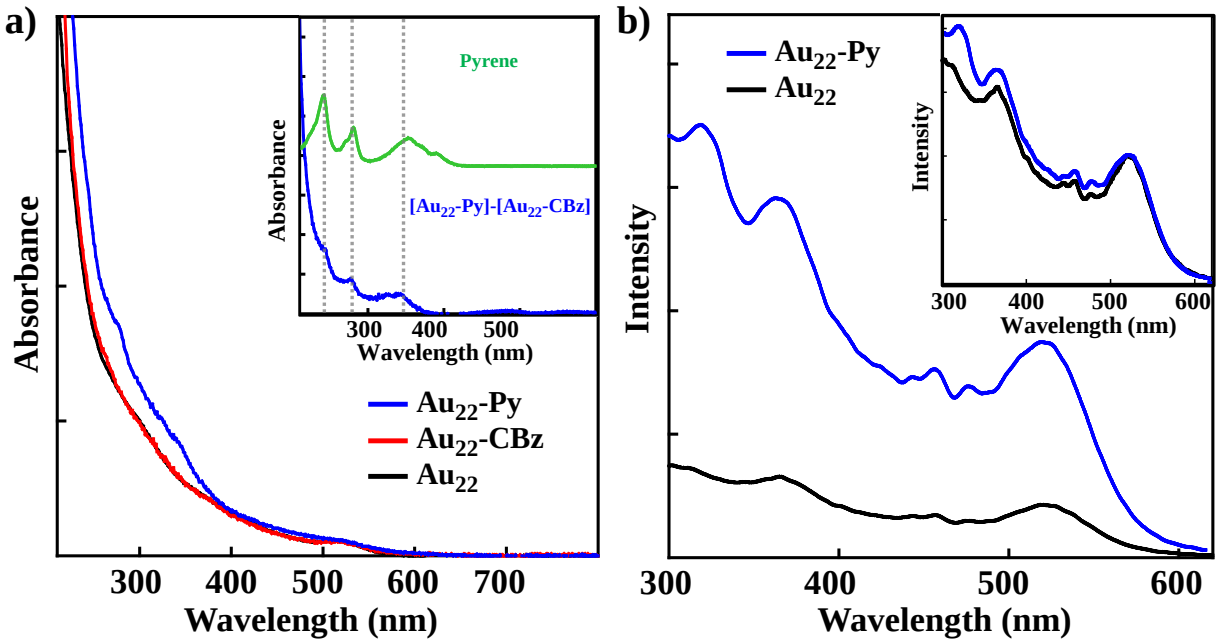

Figure S1. a) Optical absorption spectra of Au_{22}, Au_{22}-CBz and Au_{22}-Py. Inset shows the difference spectrum (blue line) obtained by subtracting the spectrum of Au_{22}-CBz from that of Au_{22}-Py. The peak positions in the difference spectrum match well with those of Py (green line). b) PL excitation spectra (λ_{EM} = 650 nm) of Au_{22} and Au_{22}-Py. Inset shows normalized (at 520 nm) PL excitation spectra of Au_{22} and Au_{22}-Py. The enhanced PL intensity at ~350 nm indicates the contribution from Py bound to Au_{22}.

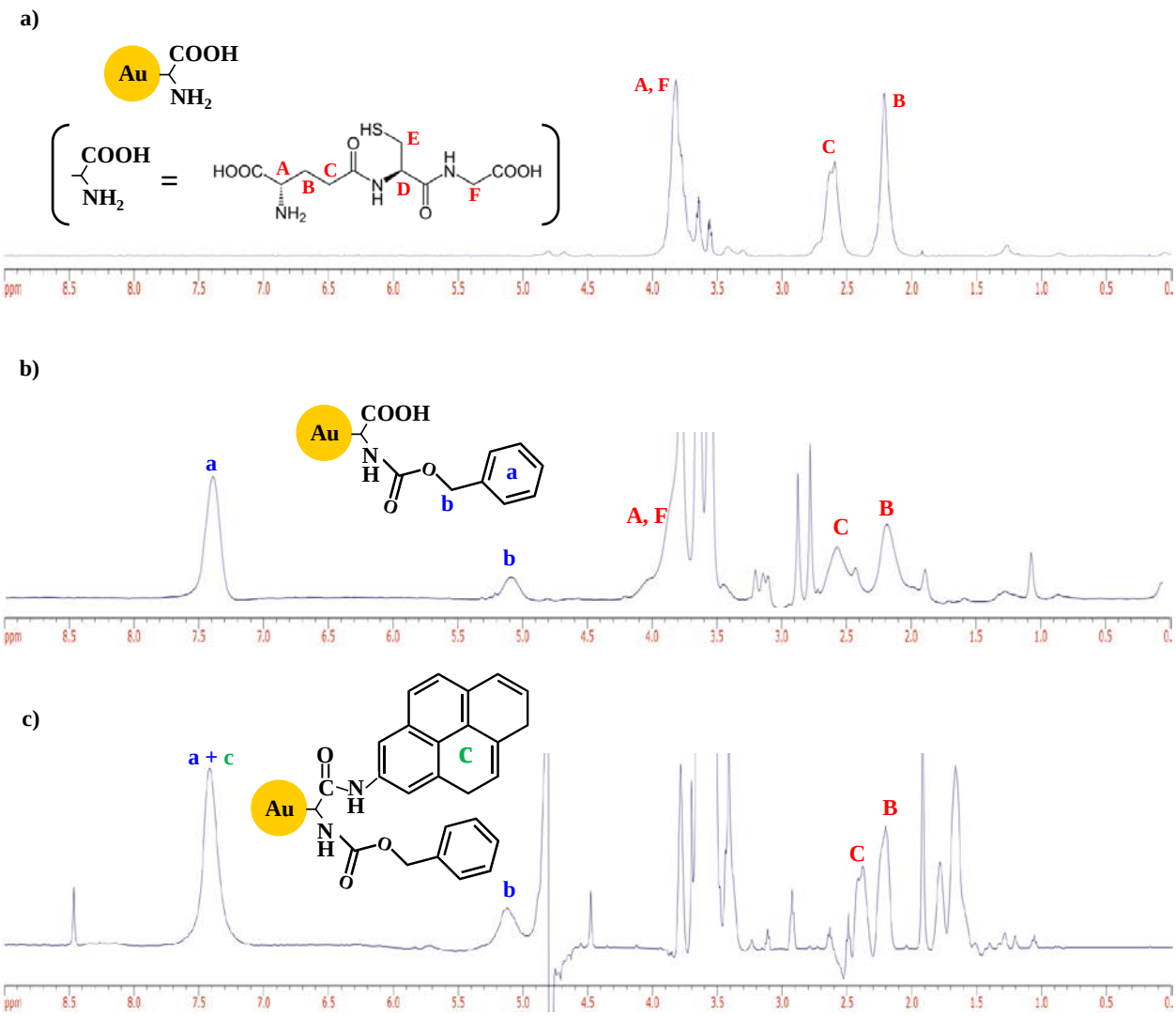

Figure S2. ^{1}H NMR spectra of a) $Au_{22}SG_{18}$, b) Au_{22}-CBz and c) Au_{22}-Py in D_2O. The number of pyrene bound to Au_{22}-CBz was determined as 2 from the peak area comparison in Figure S2c.

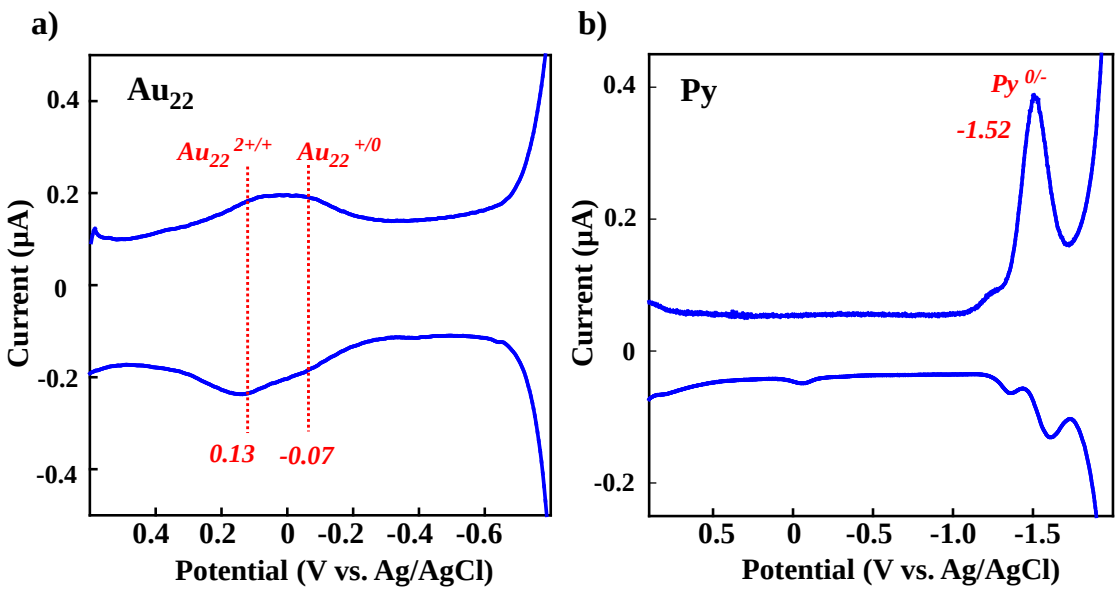

Figure S3. (a) Square wave voltammograms (SWV) of Au_{22} in 0.1 M KCl. Au_{22} clusters were ion-paired with poly(allylamine hydrochloride) and dropcast on a glassy carbon electrode to fabricate a Au_{22} modified electrode. (b) SWV of pyreneamine (Py-NH_2) in CH_2Cl_2 containing 0.1 M Bu_4NClO_4.

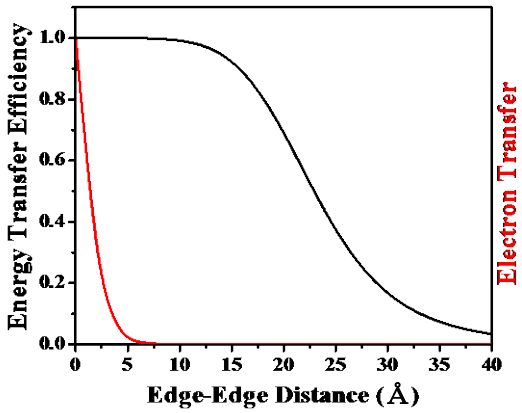

Figure S4. Au-Py distance dependent efficiencies of energy transfer (black line) and electron transfer (red line). Note that the energy transfer efficiency is plotted against the edge-to-edge distance between the donor and acceptor.

Time-resolved PL measurements

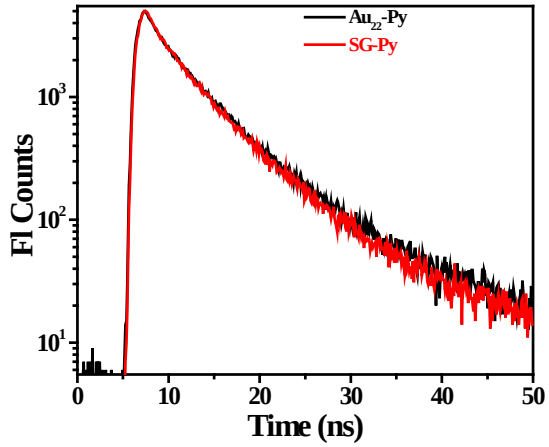

Figure S5. Nanosecond time-resolved PL decay traces at 450 nm after excitation at 373 nm with a diode laser. The decay traces do not show any appreciable changes.

Table S1. Nanosecond PL lifetimes of various Au_{22} clusters

Clusters	**Lifetimes**	**Avg lifetime**
Au_{22}	8 ns (47.6%), 180 ns (26.7%), 1200 ns (25.0%) and > 5 ms (1.0%)	350 ns
Au_{22}-CBz	160 ns (32.9%), 980 ns (37.2%), 3585 ns (29.9%)	1490 ns
Au_{22}-Py	160 ns (32.1%), 980 ns (35.4%), 3240 ns (32.5%)	1440 ns
Au_{22}-TOA	160 ns (30.7%), 980 ns (34.6%), 3580 ns (34.8%)	1730 ns

Table S2. Extinction coefficient (ε) at the excitation wavelength (λ_{EX}), quantum yield (ϕ), and brightness (εϕ) of various Au_{22} clusters

Cluster	**λ_{EX} (nm)**	**ε ($M^{-1}cm^{-1}$)**	**ϕ**	**εϕ ($mM^{-1}cm^{-1}$)**
Au_{22}	520	4199	0.055	0.23
	350	20089	0.03	0.60
Au_{22}-Py	520	4199	0.30	1.26
	350	26669	0.16	4.27
Au_{22}-Py-TOA	520	4199	0.70	2.94
	350	30756	0.28	8.61

Table S3. Time-resolved PL lifetimes after exciting pyrene

Cluster	**Lifetimes**	**Py related lifetimes**
Py	2.2 ps (growth) and decay > 1 ns	3.3 ns
Au_{22}	0.160 ps (100%)	
Au_{22}-CBz	0.170 ps (97.8%), 1.5 ps (2.2%)	
Au_{22} -Py	0.16 ps (93.8%), 1.6 ps (1.2%), 16 ps (4.2%) and >1 ns (0.8%)	1.6 ps (19.3%), 16 ps (67.7%) and 3.3 ns (12.9%) (Avg = 436 ps)
Au_{22}-Py-TOA	0.24 ps (89.4%), 35.0 ps (8.6%) and >1 ns (2.0%)	35 ps (81.1%), 3.3 ns (18.9%) (Avg = 650 ps)

Femtosecond transient absorption measurements

Shown in Figure S6 are the excited state absorption (ESA) spectra at time delays for Py after excitation at 370 nm. The transient absorption features are dominated by the single-singlet absorption at 525 nm. The decay of transients is accompanied by a vibrational cooling time constant of 11 ps and long singlet state decay.

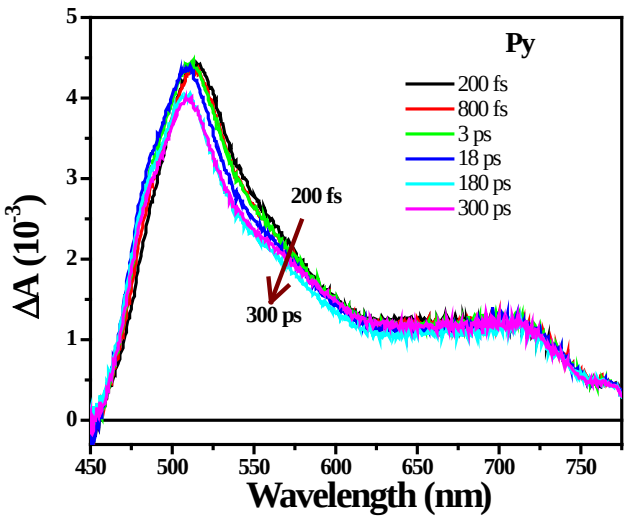

Figure S6. ESA spectra of pyreneamine (Py) in ethanol at different time delays from 200 fs to 300 ps after excitation at 370 nm.

The ESA at different time delays for Au_{22} in water after excitation at 370 nm are shown in Figure S7. The spectral features show a growth around the broad positive spectral features in the wavelength region of 550 to 700 nm and decay from 450 to 530 nm. The global fitting analysis has revealed time constants of 200 fs and long-lived transient with a maximum at 680 nm. Fast relaxation is assigned to the relaxation of core-gold states to shell-gold followed by the long-lived ESA that is assigned to the absorption of lowest excited state centered on shell-gold.

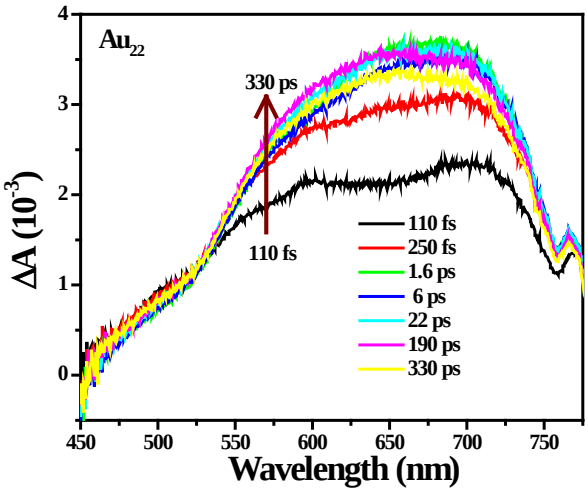

Figure S7. ESA spectra of Au_{22} in water at different time delays from 110 fs to 330 ps after excitation at 370 nm.

On the other hand, the ESA spectra of Au_{22}-Py in water shown in parts A and B of Figure S8 show a different absorption features from that of Au_{22}. A fast decay was observed as well as a growth of the transient centered at 680 nm. However, the ESA spectra show a prominent transient absorption feature centered at 495 nm that can be assigned to the anion radical of Py.[51] The presence of Py anion radical suggests that electron transfer or charge-transfer from Au_{22} to the bound Py.

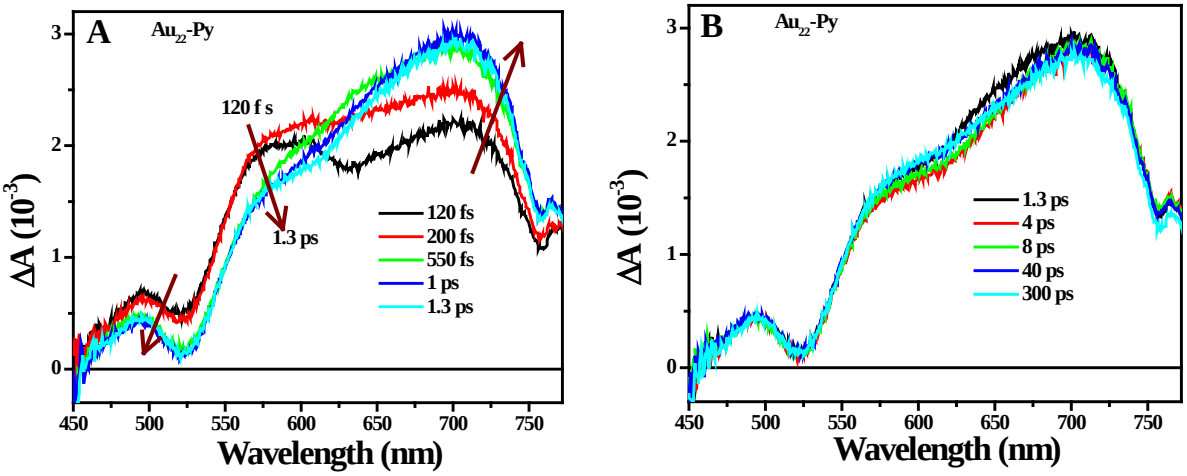

Figure S8. ESA spectra of Au_{22}-Py in water at different time delays (A) from 120 fs to 1.3 ps and (B) from 1.3 ps to 300 ps after excitation at 370 nm.

The ESA features observed for Au_{22}-TOA are quite similar to that of Au_{22} (Figure S9). The global fit analysis has shown 280 fs and >200 ps decay components that are assigned to core-gold to shell-gold relaxation followed by the relaxation of shell-gold.

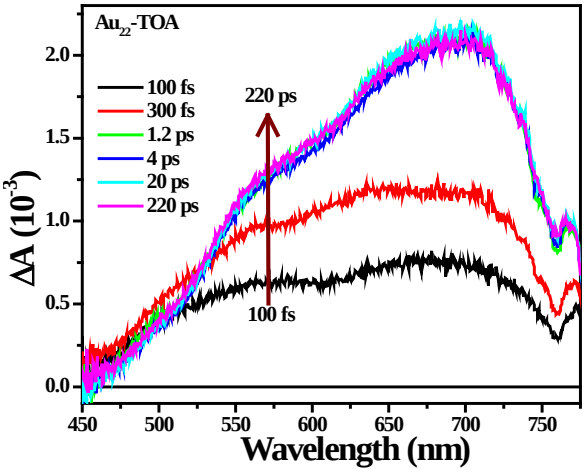

Figure S9. ESA spectra of Au_{22}-TOA in toluene at different time delays from 100 fs to 220 ps after excitation at 370 nm.

The transient absorption spectra of Au_{22}-Py-TOA at different time delays (Figures S10A and S10B) are more similar to Au_{22}-TOA than Au_{22}-Py. The peak at 495 nm is still visible that was assigned to Py anion radical but its absorbance is considerably smaller compared to Au_{22}-Py, indicating smaller contribution of electron transfer or charge transfer when the cluster is bound to TOA.

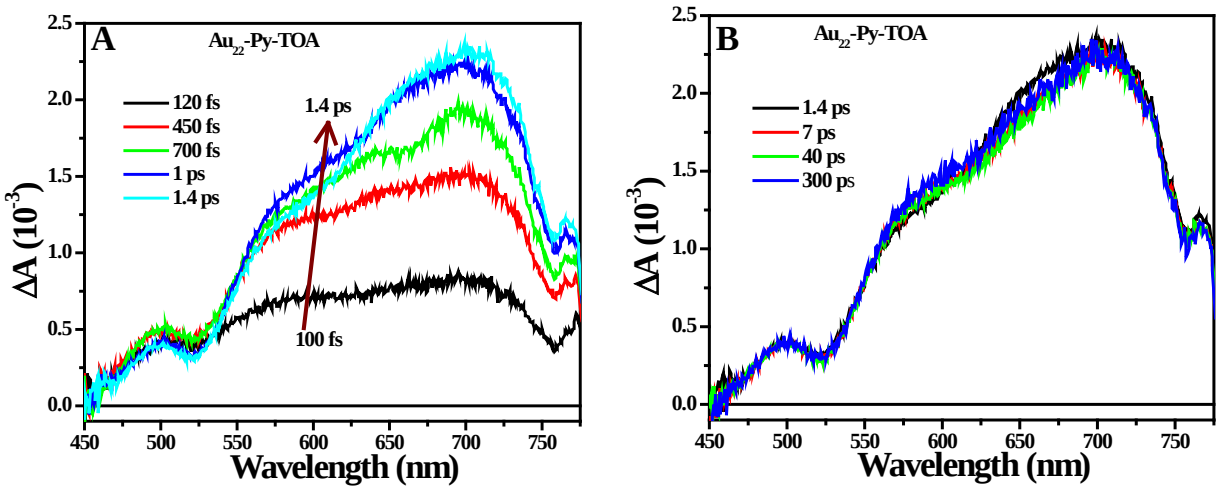

Figure S10. (A) ESA spectra of Au_{22}-Py-TOA in toluene at different time delays (A) from 120 fs to 1.4 ps and (B) from 1.4 ps to 300 ps after excitation at 370 nm.